Ain Shams Engineering Journal 14 (2023) 102343

Contents lists available at ScienceDirect

Ain Shams Engineering Journal

journal homepage: www.sciencedirect.com

Adaptive controlled superconducting magnetic energy storage devices for performance enhancement of wind energy systems

Rania A. Turky [a], Tarek S. Abdelsalam [a], Hany M. Hasanien [a,b,*], Mohammed Alharbi [c], Zia Ullah [d], S.M. Muyeen [e], Amr M. Abdeen [a]

[a] Electrical Power and Machines Department, Faculty of Engineering, Ain Shams University, Cairo 11517, Egypt
[b] Faculty of Engineering and Technology, Future University in Egypt, Cairo 11835, Egypt
[c] Electrical Engineering Department, College of Engineering, King Saud University, Riyadh 11421, Saudi Arabia
[d] School of Electrical and Electronic Engineering, Huazhong University of Science and Technology, Wuhan 430074, China
[e] Department of Electrical Engineering, Qatar University, Doha 2713, Qatar

ARTICLE INFO

Article history:
Received 3 May 2023
Revised 26 May 2023
Accepted 27 May 2023
Available online 24 June 2023

Keywords:
Adaptive control
Power systems
SMESD
Wind energy systems

ABSTRACT

This research paper introduces the Generalized Continuous Mixed P-Norm Sub-Band Adaptive Filtering (GCMPNSAF) algorithm, designed for efficient online control of Superconducting Magnetic Energy Storage Devices (SMESDs) in Wind Energy Systems (WESs). The primary objective of this algorithm is for minimizing power ripples in WESs. The Wind Energy System (WES) under consideration is tied to the IEEE 39 bus system, with the Superconducting Magnetic Energy Storage Device (SMESD) integrated at the point of common coupling. The GCMPNSAF algorithm is applied to update or adapt proportional-integral (PI) controller gains of SMESD interface circuits. The proposed algorithm is an enhanced version of the CMPN by adding the sub-band filtering algorithm effect. It depends mainly on the actuating error signal, and it has a variable step size of the CMPN. The detailed modeling of the whole system is presented, including measured wind speed data, detailed switching techniques, a drive train model of the turbine, and real SMESD. The efficacy of the proposed SMESD has been validated through a comparative analysis with the Least Mean Square-SMESD approach, under conditions of varying and unpredictable wind speeds. The simulation results produced by the PSCAD software are used to evaluate the study's validity. The utilization of controlled SMESDs has the potential to significantly enhance the power quality of WESs.

1. Introduction

1.1. Research problem

The renewable energy systems (RESs) have garnered significant interest worldwide in recent times, owing to their potential to offer sustainable and clean sources of energy. There are several reasons beyond the significant potential of the RESs, such as an surge in fuel prices, its reduction possibility, the trend toward sustainable development goals, environmental issues, and some political concerns [1]. A broad consensus is existed in promoting fast and effective decarbonization, as it was an extensive object of the Sharm El-Sheikh climate change conference (COP27). Therefore, electricity generation from RESs should push forward to satisfy economic decarbonization [2]. Wind energy conversion systems are considered the second rank of largest RESs after global hydropower. The annual global wind energy report states that new installations of 94 GW are added, and the total wind energy capacity reaches 837 GW in 2021. Based on these statistical analyses, interconnection of wind systems with power grids has reached a state of high saturation in recent times leading to arising of many problems, including power systems reliability, dynamics, stability, operation, and control. Power quality issue is considered one of the challenges face wind systems. The mechanical power of wind systems is based on the wind speed cube, and this wind speed possesses an inter-

* Corresponding author at: Electrical Power and Machines Department, Faculty of Engineering, Ain Shams University, Cairo 11517, Egypt.
E-mail address: hanyhasanien@ieee.org (H.M. Hasanien).

Peer review under responsibility of Ain Shams University.

Production and hosting by Elsevier

https://doi.org/10.1016/j.asej.2023.102343
2090-4479/

Abbreviations

ANN	Artificial neural network
CMPN	Continuous Mixed P-Norm
ESDs	Energy storage devices
FS	Fixed-speed
FLCs	Fuzzy logic controllers
GCMPNSAF	Generalized Continuous Mixed P-Norm Sub-Band Adaptive Filtering
IGBT	Insulated gate bipolar transistor
LMS	Least mean square
PLL	Phase-locked loop
PI	Proportional-integral
PCC	Point of common coupling
RESs	Renewable energy systems
SMESDs	Superconducting Magnetic Energy Storage Devices
VS	Variable-speed
VSC	Voltage source converter
WES	Wind Energy System
WT	Wind turbine

mittent and sophisticated nature profile. This is easily resulting in more output power fluctuations in wind energy systems. Generally, wind energy systems (WESs) may contain fixed-speed (FS) or variable-speed (VS) wind turbines (WTs) or both. However, FSWTs suffer from the most significant mechanical stress of their shaft, leading to a higher fluctuation in their output power generation [3]. This affects more variation of reactive power of such generators. Moreover, these power fluctuations have an adverse impact on the voltage response at the point of common coupling (PCC) of the WESs. This leads to a deep reduction in the power quality concern of such WESs. The primary aim is to achieve an efficient control of energy storage devices, with the aim of mitigating output power fluctuations and enhancing power quality of WESs.

1.2. Related works

The primary goal of many research projects has been to reduce real power ripples of WESs, enhancing the power quality concern of such renewable energy sources. It is claimed that a blade pitch angle control can help decrease such power ripples of WESs [4]. The mechanical nature of this control mechanism, however, results in a delayed response time. Additionally, if it reacts quickly to reduce these ripples, the blades will be under much compressive stress. The maximum power of WESs is tracked, and its fluctuations are decreased using the rotational inertia methodology [5]. Nevertheless, when a significant disruption occurs, it struggles with delayed transient behavior. Various RESs, including waves and wind energy conversion systems, are used to reduce active - power fluctuations during the islanded mode of operation [6]. Moreover, the ramp control approach is employed in the heat ventilation air conditioning system to regulate the active power of WESs [7]. There are many distributed generation sources like wind and photovoltaic generators cooperating together with the purpose of enhancing the active power profile [8]. Also, the energy of rotating masses of permanent magnet synchronous wind generator can be utilized in power ripples minimization of WESs [9], but the scientific model of the scheme does not consider uncertainty effects. In [10], a fuzzy logic control scheme with the help of a low pass filter to enhance power responses. Moreover, a classical approach is implemented to reduce the power ripples of WESs declining system disturbances, but it depend on on a linear model for the system [11]. In [12], The model predictive controller has been employed in order to effectively mitigate output power fluctuations in WESs, and it depends on a quadratic programming approach. However, like all conventional optimization methods, it relies on initial conditions, solver accuracy, and may stuck into local minima point. A two-layer control scheme was recently proposed to optimize power balance between generation and load demand, while also enhancing the wind power profile. However, the procedure involved in this approach is complex and time-consuming [13]. The hydrogen system is used to stabilize wind power fluctuations [14].

The integration of storage devices with WESs has a high influence on the overall effectiveness of active power smoothing techniques. Battery energy storage devices (ESDs) are extensively used to minimize power fluctuations of WESs. In [15], comprehensive reviews and surveys of various control techniques of batteries are demonstrated to minimize power ripples of such systems. Effective control of the battery system is crucial for optimizing the system cost. The dual batteries ESDs are implemented to smooth WESs power fluctuations with better economic benefits [16]. In [17], a wavelet analysis method is proposed for battery ESDs to investigate different components of power ripples. In addition, battery ESDs can be sized based on the model predictive control scheme to minimize power ripples of WESs [18]. A deep reinforcement learning methodology is proposed to control wind energy systems with battery ESDs to achieve the same target [19]. In [20], the impact of battery ESDs on power ripple minimization of WESs is investigated by considering the initial value of the state of charge, switching frequency, and high pass filters. Although the battery ESD is a more cost-effective device, it has numerous drawbacks, including its delayed response time due to chemical processes, the constraints on voltage and current, and its negative environmental impact. Despite the high cost of supercapacitor systems, these are widely used to minimize power ripples and enhance the dynamic responses of wind energy systems [21–23]. In addition, flywheel ESDs are considered a candidate solution to smooth power ripples of WESs. In this regard, flywheel ESDs have various advantages, including reduced cost, greater power capacity, more reliability, true transient performance, and longer lifespans [24–26]. Despite the merits of flywheel ESDs, these suffer from high friction and windage losses leading to a lower efficiency [3]. On the other hand, superconducting magnetic ESDs (SMESDs) represent adequate storage devices for power ripples minimization of WESs. SMESDs possess several merits, like high efficiency [27], quick transient behavior [28], and unlimited cycles of charging/discharging processes [29]. The cost of superconducting material plays an important role in this industry, and there are many research funds oriented toward decreasing the material cost [30,31]. Various controllers have been implemented to control SMESDs. To enhance the efficiency of photovoltaic power plants, SMESDs are controlled by fuzzy logic controllers (FLCs) [32]. Moreover, FLCs are utilized to control SMESDs with the purpose of improving the microgrids stability [29]. Although FLCs work with the nonlinearity of the system and no need to a system model, they rely on fuzzy rules and gains that are appropriately designed. In addition, an artificial neural network (ANN) control strategy is applied to SMESDs to enhance the stability of WESs [33,34]. Despite the merits of ANN controllers that deal with the system's nonlinearity, they establish complex structures and require a long time to perform training and testing processes. Proportional-Integral (PI) controllers are widely utilized in various applications

in modern times. This is a result of its broad stability range and low-cost applications. The systems nonlinearity, unpredictability, and susceptibility to parameter modification, however, are drawbacks. In order to obtain optimal gains for PI controllers, especially for complex, nonlinear systems where transfer functions or state space models are complex to obtain, various metaheuristic optimization algorithms are employed for their design [35–39]. Although these approaches are useful and excellent tools for designing PI controllers, they have several drawbacks, such as a complicated methodology, a heavy memory requirement, and a lengthy optimization phase. Adaptive PI controllers are strong choices for online tuning of controller gains, as a consequence, optimization procedures are not required. This helps in cutting down on the time and effort needed for the lengthy design process. Several adaptation techniques, including adaptive weight algorithm [40], affine projection [41], and variable mixing norm [42], were employed to update PI controller gains. The tremendous development of adaptive filtering algorithms, including a quick and accurate response, represents the principal incentive of the authors to utilize a generalized continuous mixed p-norm sub-band adaptive filtering (GCMPNSAF) algorithm to fully control SMESDs for minimizing power ripples of WESs.

1.3. Main contribution

Numerous technical issues, such as those involving communications and signals, have been successfully solved by the adaptation methods and associated algorithms [43,44]. Adaptive Filtering Algorithms (AFAs) typically rely on an error signal, which represents the difference between a reference signal and the actual output signal. Most AFAs depend on the concept of least mean square (LMS) error [45]. In addition, some approaches rely on the error signal's p-norm [46]. The utilization of AFAs has been widely adopted to improve the dynamic performance of Renewable Energy Systems [47,48]. It is essential to find the right balance between an algorithm's accuracy and complexity. Therefore, in this article, an intelligent GCMPNSAF algorithm is presented. The proposed algorithm is an improved version of the CMPN algorithm, achieved through the incorporation of sub-band filtering techniques. It depends mainly on the actuating error signal, and it has a variable step size of the CMPN [49]. The GCMPNSAF algorithm possesses various advantages over other AFAs, such as individual weight factor SAF, normalized logarithmic SAF, and improved proportionate normalized SAF [49]. Some benefits of the GCMPNSAF include quick convergence, a straightforward process, and less complicated computing. Therefore, the GCMPNSAF algorithm is implemented in this study to automatically adapt PI controllers gains of SMESDs with the determination of flattening the output power of WESs.

The current study involves the connection of a WES to the IEEE 39 bus New England system, with a SMESD tied to the WES at the point of common coupling (PCC). A VSC is employed within the SMESD to effectively control both PCC and DC-link voltages, with an additional DC chopper circuit utilized to regulate the active power of the SMESD. The proposed adaptive PI controllers are responsible for controlling the converters. In order to achieve realistic results, actual wind speed data obtained from Hokkaido Island is used for dynamic simulations. The WT model is thoroughly considered and actual SMESD is utilized, with simulation analyses performed through the use of PSCAD software [50]. The validity of the controlled SMESD is established by conducting a comparative analysis of its results with those obtained using other methods, particularly under the nonlinearity conditions of the system under study. The active power output from the WES can be made more uniform and their ripple can be significantly reduced with the adoption of the suggested control approach, enhancing the power quality of WESs.

The paper organization is done as follows: System modeling is demonstrated in Section 2. The WES model is introduced in Section 3. A SMESD control strategy is demonstrated in Section 4. The GCMPNSAF algorithm is fully detailed in Section 5. The findings are illustrated in Section 6, with a focus on research. Finally, Section 7 brings study conclusions.

2. The system model

The power network chosen for this investigation is the IEEE 39 bus standard system. It illustrates the New England power network in a small form. Utilizing such massive systems is done primarily to provide a realistic evaluation of the WES. The graphical representation of such system is shown in Fig. 1 [3]. It contains 39 buses and there are 19 load buses. Bus 31 is known as the slack-bus and the system has 10 generators. Active power for the load and generation is 6098.1 and 6140.81 MW, respectively. As a choice for load modeling, constant current and admittance is used. The generators' active power output varies from 250 to 1000 MW. A 10 MW WES is tied to bus 30 as well as the synchronous generator number 10, which provides 240 MW. The proposed controlled SMESD is connected to the WES PCC. The statistics for generators, buses, and loads are shown in Tables 1-3, respectively [3].

3. The WES modelling

The following mathematical formulas can be used to express the mechanical power obtained from wind turbines (WTs) [33]:

$$P_M = 0.5\rho\pi R^2 V_W^3 C_P(\lambda,\beta) \tag{1}$$

where P_M stands for mechanical power of a WT, ρ is the air density, R is the radius of a WT, V_W represents the wind velocity. Power coefficient (C_p) is expressed by tip-speed ratio λ and blade angle β as follows:

$$C_p = 0.5\left(\lambda_i - 0.022\,\beta^2 - 5.6\right)e^{-0.17\lambda_i} \tag{2}$$

$$\lambda = \frac{\omega_B R}{V_W}, \lambda_i = \frac{3600\,R}{1609\,\lambda} \tag{3}$$

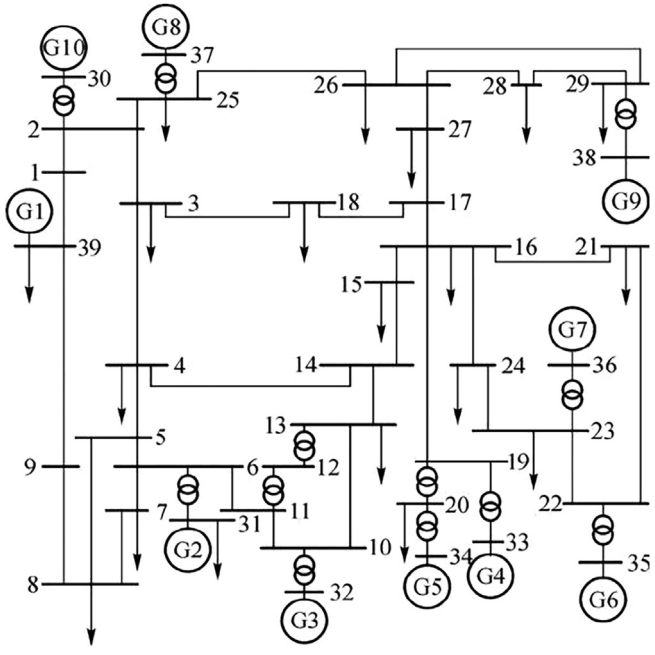

Fig. 1. IEEE 39 bus system.

Table 1
Generators Data.

Bus	Total apparent Power (MVA)	Generated real power (MW)	Bus voltage(p.u)
30	289.590	250	1.04750
31	557.270	520.810	0.9820
32	681.600	650	0.98310
33	641.490	632	0.99720
34	534.360	508	1.01230
35	683.830	650	1.04930
36	569.070	560	1.06350
37	540	540	1.02780
38	830.310	830	1.02650
39	1003	1000	1.030

In (3), ω_B stands for an angular velocity of a WT. The three-drive train model is implemented to represent WTs and it provides a high level of accuracy and has a significant impact on transient responses. Its detailed characteristics are demonstrated in Table 4. Inertia constants of a wind turbine, gear box and generator are represented by H_{WT}, H_{GB}, and H_G. Parameters K_{HGB} and K_{GBG} stands for shaft spring constant between hub-gear box and gear box-generator, respectively. D_{WT}, D_{GB}, and D_G devotes self-damping coefficient of such components. d_{HGB} and d_{GBG} represents mutual damping between them. The WES consists of five squirrel cage induction generators having a rated power of 2 MVA each.

Table 2
Buses Data.

Bus	Bus name	Base kV	Voltage magnitude (p.u)	Voltage angle (degree)
1	1	345	1.04500	−8.5400
2	2	345	1.04100	−5.8200
3	3	345	1.02500	−8.6800
4	4	345	1.00100	−9.6800
5	5	345	1.00300	−8.6700
6	6	345	1.00600	−8.0100
7	7	345	0.99500	−10.1900
8	8	345	0.99400	−10.6900
9	9	345	1.02800	−10.4100
10	10	345	1.01500	−5.4800
11	11	345	1.01100	−6.3400
12	12	345	0.99800	−6.3100
13	13	345	1.01200	−6.1600
14	14	345	1.00900	−7.7200
15	15	345	1.01300	−7.7900
16	16	345	1.02900	−6.2300
17	17	345	1.0300	−7.3400
18	18	345	1.02700	−8.2800
19	19	345	1.04900	−1.0600
20	20	345	0.99100	−2.0500
21	21	345	1.0300	−3.8200
22	22	345	1.04900	0.6400
23	23	345	1.04400	0.4400
24	24	345	1.03500	−6.1100
25	25	345	1.04400	−4.1800
26	26	345	1.04500	−5.4700
27	27	345	1.03200	−7.4900
28	28	345	1.04700	−1.9300
29	29	345	1.04800	0.8400
30	Gen 10	22	1.04800	−3.3900
31	Gen 2	22	0.98200	0.0
32	Gen 3	22	0.98300	2.5100
33	Gen 4	22	0.99700	4.1600
34	Gen 5	22	1.01200	3.1400
35	Gen 6	22	1.04900	5.5900
36	Gen 7	22	1.06400	8.300
37	Gen 8	22	1.02800	2.5100
38	Gen 9	22	1.02700	7.9100
39	Gen 1	345	1.0300	−10.1500

4. SMESD and its control circuits

As an energy storage device in power or renewable energy systems, SMESD has beneficial properties including high efficiency, rapid reaction, no degradation during repeated operation, and more. Then, a wide range of SMESD applications are anticipated. Nevertheless, it includes multiple issues like reliability verification and lowering costs for effective SMESD utilization. There are numerous initiatives worldwide to develop SMESDs. In this paper, a practical SMESD is connected to the WES PCC. Nominal power and energy storage of the SMESD is 10 MW and 20 MJ, respectively. It was successfully installed at t at Hosoo power plant, Japan [51]. It consists of a three-phase transformer, VSC, DC link capacitor, a DC chopper circuits and superconducting coil. The DC link capacitor has a capacitance of 15 mF. The SMESD coil has a self-inductance L_s of 21.1H. The SMESD components are demonstrated in Fig. 2. Stored energy E_s of SMESD and its nominal power P_s is written by the following formulas:

$$E_s = 0.5 L_s I_s^2 \tag{4}$$

$$P_s = \frac{dE_s}{dt} = L_s I_s \frac{dI_s}{dt} = V_s I_s \tag{5}$$

where I_s and V_s are the coil instantaneous current and voltage.

4.1. Voltage source converter

In Fig. 2, the voltage source converter (VSC) is presented. It is a three-phase converter with six IGBTs. The VSC control is based on a cascaded control scheme, as shown in Fig. 3. There are two adaptive PI controllers located in outer loops to regulate V_{PCC} and V_{DC}. In addition, there are two adaptive PI controllers located in inner loops to regulate direct and quadrature (dq) axis currents. The V_{PCC} is measured to feed a phase-locked loop (PLL) system, which extracts an angle θ_s. This angle is essential for the abc-dq0 frames conversion. To create the firing pulses of IGBTs, $V_{a,b,c\text{-}n}$ are compared with a triangle signal with a 1.2 kHz frequency.

Table 3
Loads Data.

Bus No.	Load real power (MW)	Load reactive power (Mvar)
3	322	2.40 0
4	500	184
7	233.80	84
8	522	176
12	8.5	88
15	320	153
16	329	32.30 0
18	158	30
20	628	103
21	274	115
23	247.50	84.600
24	308.6 0	−92
25	224	47.20 0
26	139	17
27	281	75.500
28	206	27.60 0
29	283.50	26.90 0
31	9.2 0	4.60 0
39	1104	250

Table 4
WTs Characteristics.

H_G (s)	0.14190	D_{WT} (pu)	0.0220
H_{GB} (s)	0.08060	D_{GB} (pu)	0.0220
H_{WT} (s)	1.92770	D_G (pu)	0.010
K_{HGB} (pu)	54.750	d_{HGB} (pu)	3.50
K_{GBG} (pu)	1834.10	d_{GBG} (pu)	10

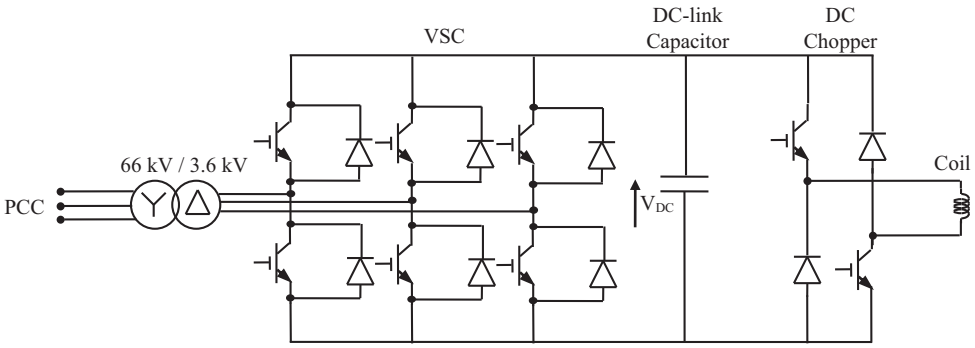

Fig. 2. SMESD components.

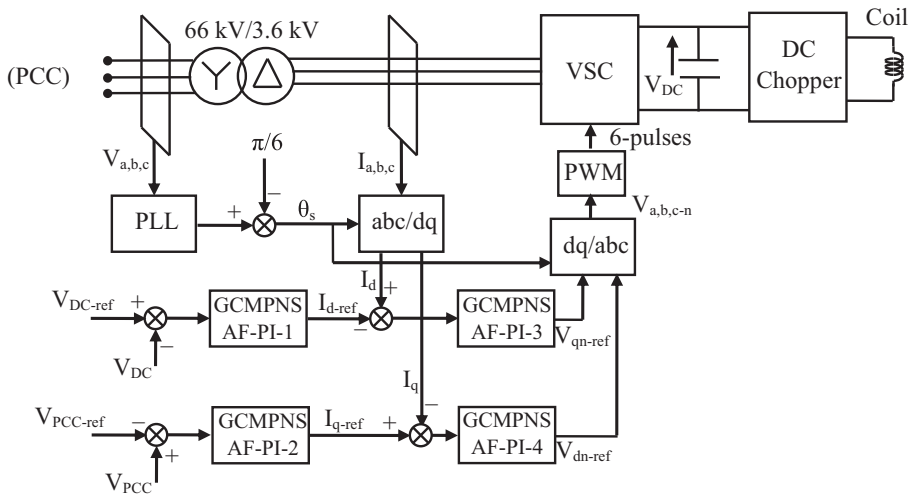

Fig. 3. VSC control scheme.

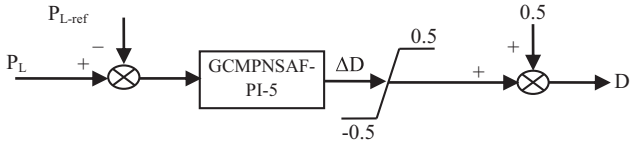

Fig. 4. DC chopper circuit control.

4.2. DC chopper circuit

A two-quadrant DC-DC converter is used in this SMESD to control the active power at the PCC (P_L). A control strategy depends on adjusting chopper duty cycle (D), where it lies in the range [0, 1] to carry out chopper cycles of SMESD. Hence, one adaptive PI controller is used to regulate P_L to its reference value $P_{L\text{-ref}}$. Fig. 4 points out the DC chopper circuit control. Lastly, the duty cycle signal enters a PWM control circuit to generate delaying pulses of IGBTs [33].

5. AFAs

5.1. GCMPNSAF algorithm

Mixed-norm adaptive filters are a class of AFAs that come in a number of variations. There is some combination between AFAs like least mean square (LMS) with least mean fourth to produce a LM mixed-norm or LMMN algorithm [52]. Also, a LMS is combined with a least absolute deviation to form the robust MN algorithm [53]. Hence, the robust normalization MN algorithm is presented [54] and it relies on error norm minimization approach by:

$$C(k) = L(k)E\{er^2(k)\} + (1 - L(k))E\{|er(k)|\} \tag{6}$$

where $C(k)$ stands for the objective function, k represents an iteration index, $L(k)$ represents parameter varying from 0 to 1. $er(k)$ represents an error signal of the AFA by:

$$er(k) = d(k) - y(k) \tag{7}$$

$$y(k) = x^T(k)we(k) \tag{8}$$

where $y(k)$ stands for the AFA output vector, $x(k)$ represents the input vector, $d(k)$ represents the reference signal vector, and $we(k)$ represents a present weight vector of AFA [45]. In [55], a p-norm strategy is applied to LMS and the standard norm is 2. The CMPNAFA is further developed and is modeled as follows [46]:

$$C(k) = \int_1^2 L_k(p)\, E\{|er(k)|^p\}\, dp \tag{9}$$

where $L_k(p)$ devotes to the probability function and its constraints are expressed as follows:

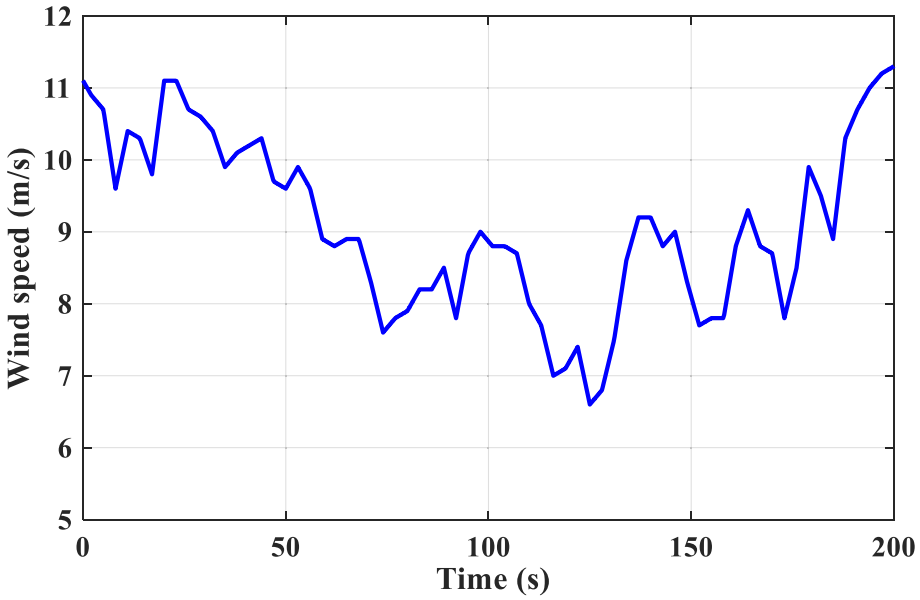

Fig. 5. Wind speed profile.

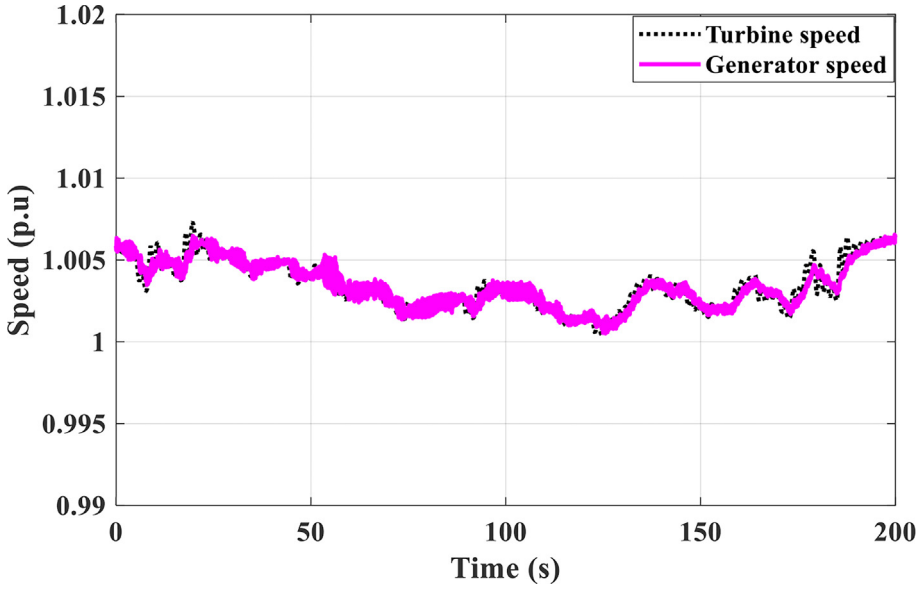

Fig. 6. Wind turbine and generator speed profile.

$$\int_1^2 L_k(p)dp = 1 \tag{10}$$

Weight vector of CMPNAFA can be updated by the following formula:

$$we(k+1) = we(k) - \mu \nabla_{we(k)} C(k) \tag{11}$$

where μ represents a step size. $\nabla_{we(k)}C(k)$ is mathematically expressed as follows:

$$\frac{\partial C(k)}{\partial we_i(k)} = \int_1^2 L_k(p) \frac{\partial}{\partial we_i(k)} E\{|er(k)|^p\}\, dp \tag{12}$$

The expectation $E\{|er(k)|^p\}$ can be approximately equal to $|er(k)|^p$. Then, the weight vector of CMPNAFA can be developed by:

$$we(k+1) = we(k) + \mu\, \gamma_k sign(er(k))x(k) \tag{13}$$

$$\gamma_k = \int_1^2 p\, L_k(p)\, |er(k)|^{p-1}\, dp \tag{14}$$

where γ_k represents a variable-step size and can be written as follows:

$$\gamma_k = \frac{(2|e(k)|-1)\ln(|e(k)|) - |e(k)| + 1}{(\ln(e(k)))^2} \tag{15}$$

Therefore, in this article, an intelligent GCMPNSAF algorithm is presented. The proposed algorithm is an enhanced version of the CMPN by adding the sub-band filtering algorithm effect. It depends mainly on the actuating error signal and it has a variable step size of the CMPN [49]. The GCMPNSAF algorithm possesses various advantages over other AFAs such as individual weight factor SAF,

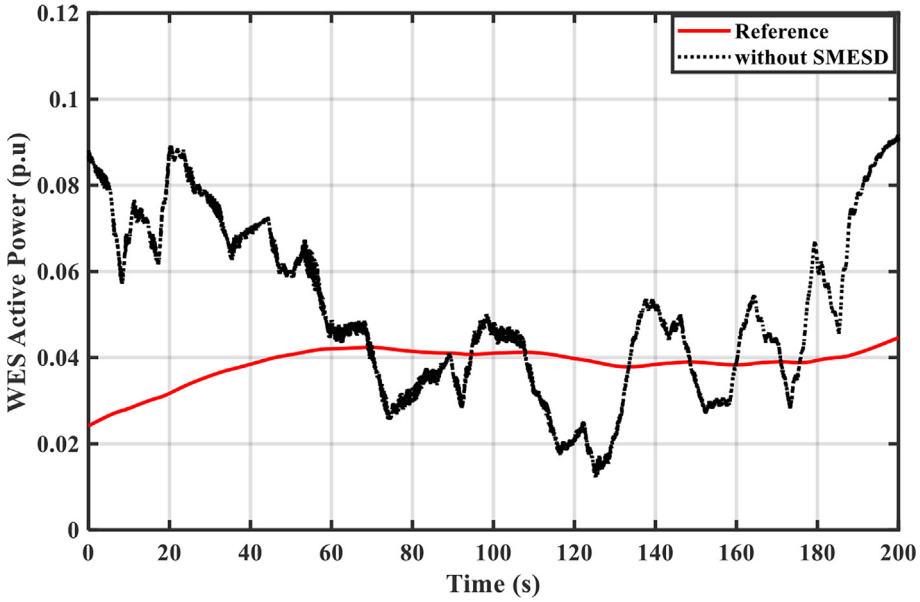

Fig. 7. WES active power.

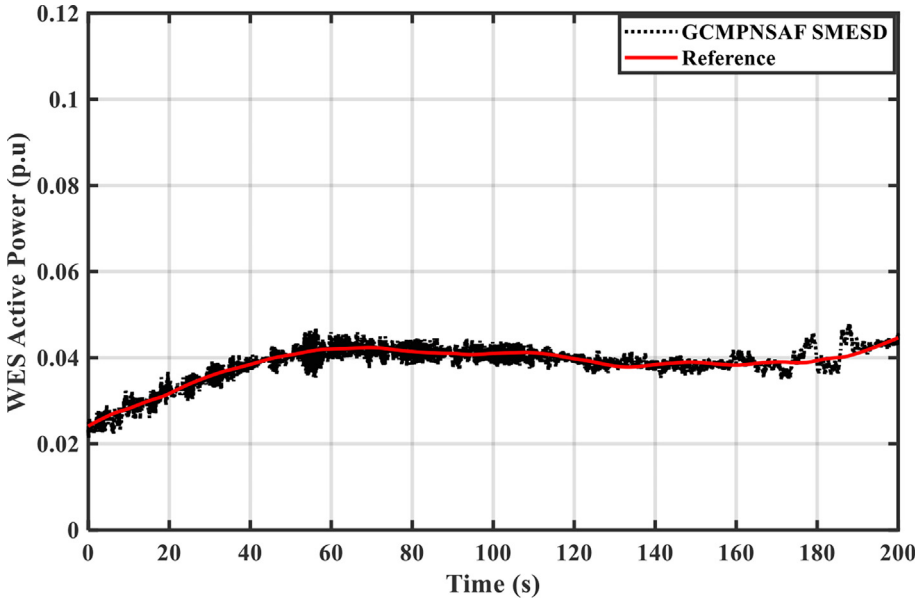

Fig. 8. WES active power using the proposed GCMPNSAF controlled SMESD.

normalized logarithmic SAF, and improved proportionate normalized SAF [49]. Some benefits of the GCMPNSAF include quick convergence, a straightforward process, and less complicated computing. The weight vector of the GCMPNSAF algorithm can be written as follows:

$$we(k+1) = we(k) + \frac{\mu\,\gamma_k sign(er(k))x(k)}{\sqrt{x^T(k)x(k)+\gamma_k}} \tag{16}$$

In this article, the controllers gains of the SMESD are adapted instantaneously by (16). $k_p(k)$ and $k_i(k)$ is adapted as follws:

$$k_p(k+1) = k_p(k) + \Delta k_p(k) \tag{17}$$

$$k_i(k+1) = k_i(k) + \Delta k_i(k) \tag{18}$$

$$\Delta k_p(k) = \Delta k_i(k) = \frac{\mu\,\gamma_k sign(er(k))x(k)}{\sqrt{x^T(k)x(k)+\gamma_k}} \tag{19}$$

where $e(k)$ is an input signal to the adaptive PI controller and $x(k)$ stands for an real signal. The initial conditions and controllers parameters are chosen to maintain the system stability.

5.2. LMS algorithm

One of the fundamental AFAs is the traditional LMS method. It has a relatively straightforward structure and uses less processing steps [3]. These characteristics, however, have an impact on performance and do not guarantee getting superior outcomes. It is based on an error signal to adapt the weight vector of the AFA and can be written by:

$$we(k+1) = we(k) + \mu\, er(k)\, x(k) \tag{20}$$

where μ is equal to 0.012. Controllers gains are updated by:

$$\Delta k_p(k) = \Delta k_i(k) = \mu\, er(k) x(k) \tag{21}$$

In this paper, a SMESD controlled by adaptive LMS-PI controllers are effectively compared with the proposed adaptive GCMPNSAF-PI controllers under the WES variability and uncertainty.

6. Simulation results and discussion

In this study, a 10 MW WES is tied to bus 30 as well as the synchronous generator number 10, which provides 240 MW. The proposed controlled SMESD is connected to the WES PCC. The detailed modeling is applied to all components, including wind turbines, wind generator, and power converters. The detailed modeling of electronic switches is considered. The simulation analyses are conducted using PSCAD software, which is well-suited for conducting transient analyses in power system studies. Simulation time interval and simulation run is chosen 10 μs and 200 s, respectively. To ensure a realistic study, the WES model incorporates measured wind speed data obtained from Hokkaido Island, as illustrated in Fig. 5, where it has a wide range variation from 6.6 to 11.3 m/s. Fig. 6 demonstrates the wind turbine and generator speeds profile. It can be realized that the generator speed exceeds the synchronous speed and lies in a satisfactory range. The WES desired active power ($P_{L\text{-}ref}$) and the active power without using SMESD are shown in Fig. 7. $P_{L\text{-}ref}$ is determined by following the generator power on a low pass filter. The WES active power using adaptive SMESD based on the GCMPNSAF and the LMS algorithms are illustrated in Figs. 8 and 9, respectively. It is noteworthy that the proposed technology achieves better damping of active power ripples in WES with minimum fluctuations compared to the LMS technology. Such power ripple is minimized by 15% at specific times using the proposed technology. The SMESD active power is demonstrated in Fig. 10, which indicates the dynamic interaction between the SMESD and the grid through the charging and discharging stages of the storage device. To evaluate the power quality, the

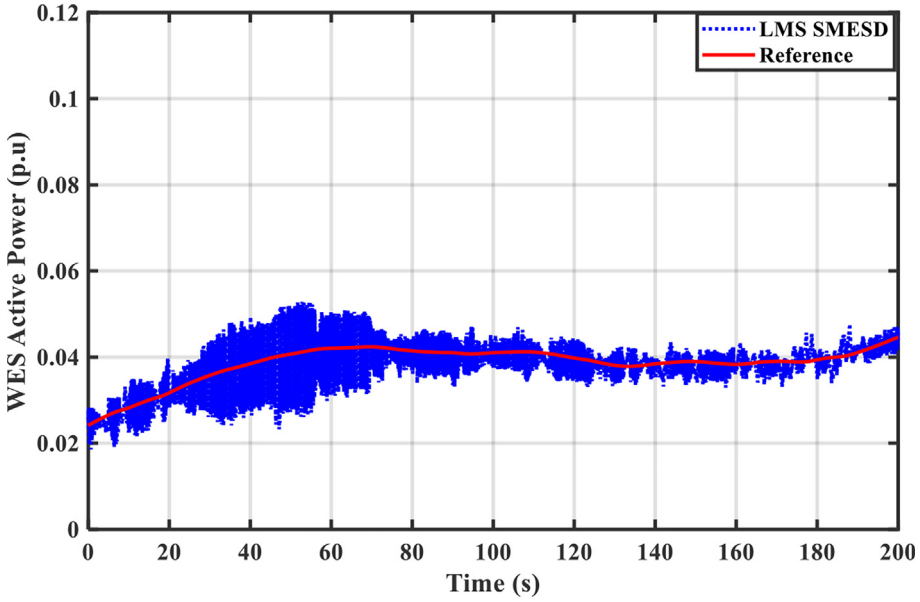

Fig. 9. WES active power using the LMS controlled SMESD.

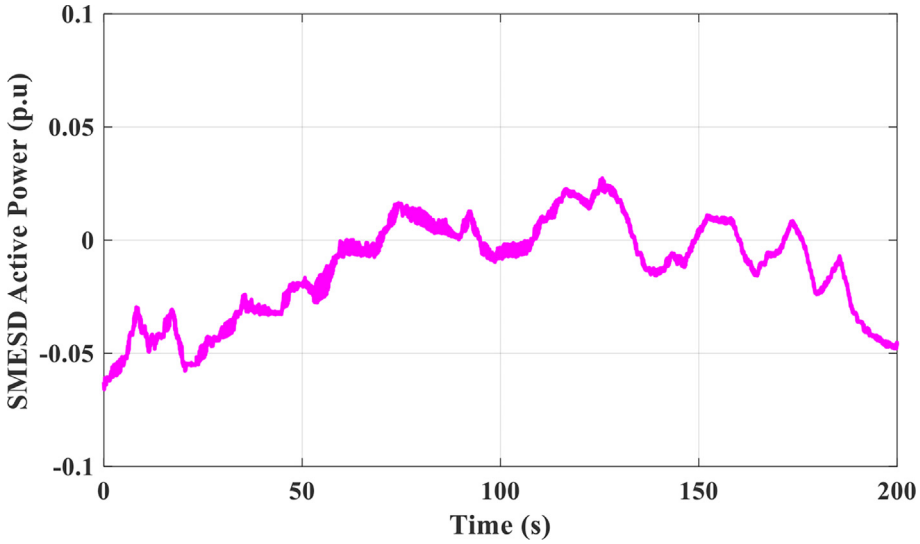

Fig. 10. SMESD active power.

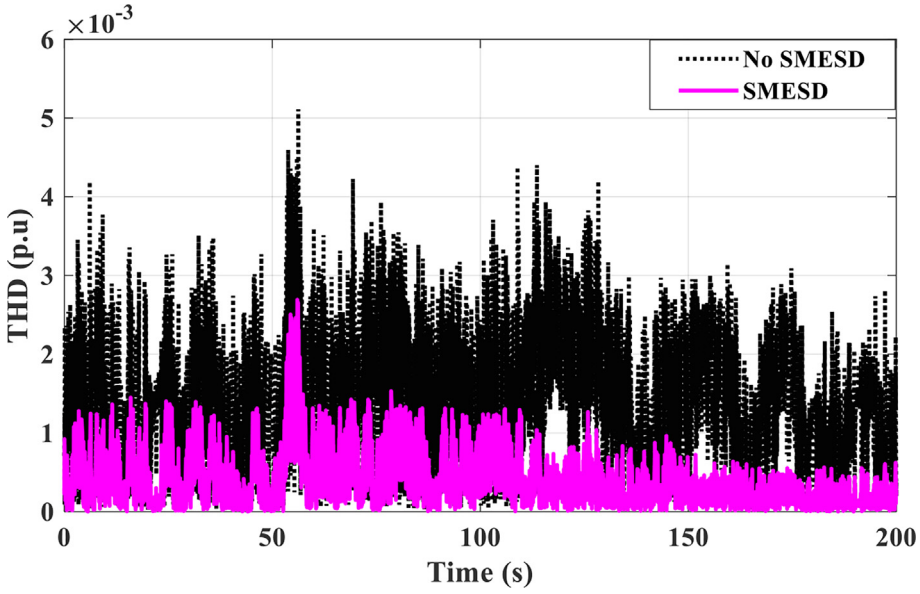

Fig. 11. THD of WES active power.

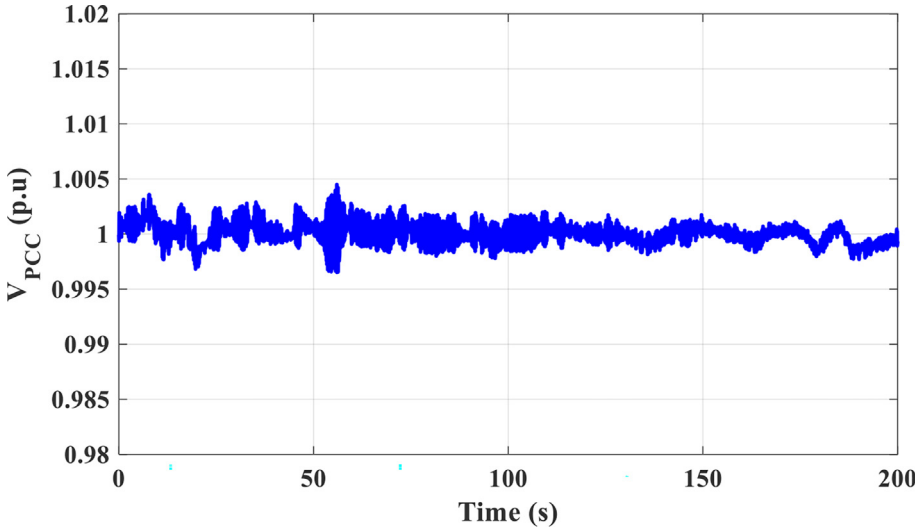

Fig. 12. V_{PCC} response.

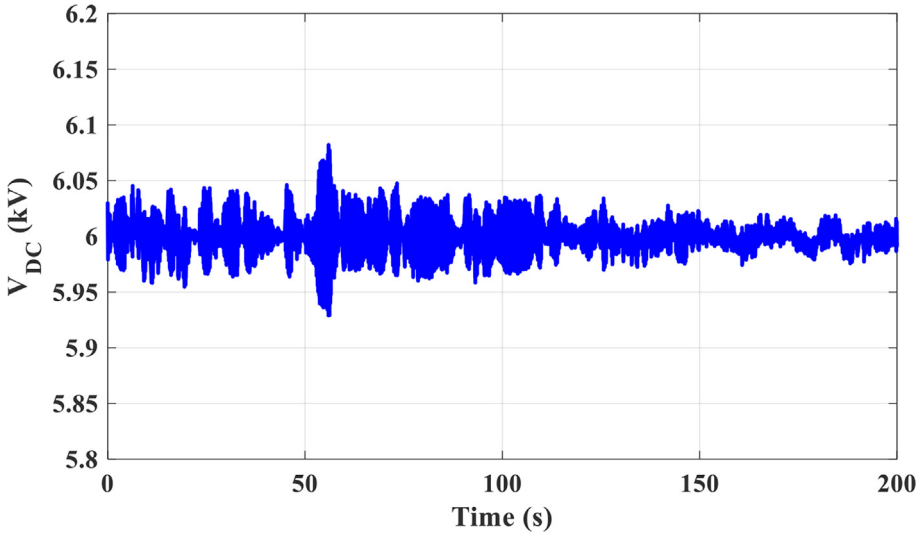

Fig. 13. V_{DC} response.

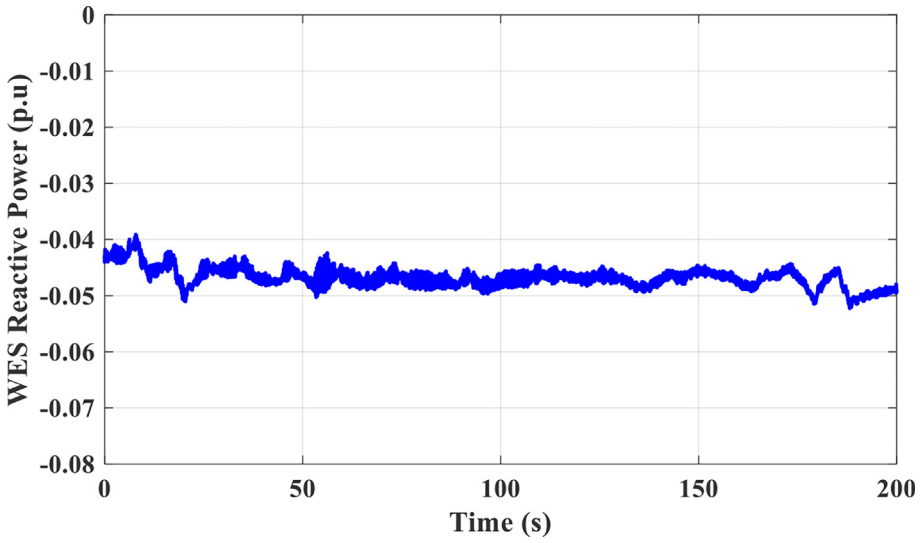

Fig. 14. WES reactive power response.

total harmonic distortion (THD) factor is analyzed for the active power response. Fig. 11 depicts the THD value of active power with and without SMESD. Notably, its value is significantly lower than that achieved without SMESD. This leads to a power quality improvement of the WESs. The V_{PCC} response is effectively adjusted to the nominal value using the controlled SMESD under wind speed uncertainty and variability, as illustrated in Fig. 12. Moreover, Fig. 13 shows the V_{DC} response of SMESD and it is kept at its rated value. The WES reactive power is plotted in Fig. 14 and it can be noted that this reactive power is supported from the SMESD. Therefore, the implementation of adaptive controlled SMESDs shall smooth the WES active power and enhance its power quality issue.

7. Conclusion

This paper has presented a novel GCMPNSAF algorithm to fully online control SMESDs for minimizing power ripples of WESs. The proposed WES is connected to the IEEE 39 bus system and the SMESD is tied to the point of common coupling. The GCMPNSAF algorithm is applied to adapt all PI controller gains of SMESD interface circuits. The proposed algorithm is an enhanced version of the CMPN by adding the sub-band filtering algorithm effect. It depends mainly on the actuating error signal and it has a variable step size of the CMPN. The detailed modeling of the whole system is presented, including measured wind speed data, detailed switching techniques, drive train model of turbine, and real SMESD. The simulation results have verified outperform of the proposed SMESD technology over that obtained using the LMS-SMESD technology under the system nonlinearity and uncertainty. The power ripple of the WES is minimized by 15% at specific times using the proposed technology. The proposed control scheme is fully adaptive and there is no need to any optimization methods leading to saving of time and efforts. The proposed technology can help in smoothing the WES active power and enhancing the system power quality. It shall be applied to several microgrids and smart grid applications. Moreover, the developments of adaptive algorithms will be extensively applied to power systems control and dynamics.

Declaration of Competing Interest

The authors declare that they have no known competing financial interests or personal relationships that could have appeared to influence the work reported in this paper.

Acknowledgement

This work was supported by the Researchers Supporting Project number (RSP2023R467), King Saud University, Riyadh, Saudi Arabia.

References

[1] Zhang Yi, Cheng C, Yang T, Jin X, Jia Z, Shen J, et al. Assessment of climate change impacts on the hydro-wind-solar energy supply system. Renew Sustain Energy Rev 2022;162:112480.
[2] "Global Wind Report 2022 - Global Wind Energy Council." https://gwec.net/global-wind-report-2022/ [accessed Jan. 09, 2023].
[3] Hasanien HM, Tostado-Véliz M, Turky RA, Jurado F. Hybrid adaptive controlled flywheel energy storage units for transient stability improvement of wind farms. J Energy Storage Oct. 2022;54:. doi: https://doi.org/10.1016/J.EST.2022.105262105262.
[4] Uehara A, Pratap A, Goya T, Senjyu T, Yona A, Urasaki N, et al. A coordinated control method to smooth wind power fluctuations of a PMSG-Based WECS. IEEE Trans Energy Convers 2011;26(2):550–8.
[5] Varzaneh SG, Gharehpetian GB, Abedi M. Output power smoothing of variable speed wind farms using rotor-inertia. Electr Power Syst Res Nov. 2014;116:208–17. doi: https://doi.org/10.1016/J.EPSR.2014.06.006.
[6] Astariz S, Iglesias G. Output power smoothing and reduced downtime period by combined wind and wave energy farms. Energy Feb. 2016;97:69–81. doi: https://doi.org/10.1016/J.ENERGY.2015.12.108.
[7] Abou Daher N, Raoofat M, Saad M, Mougharbel I, Asber D, Beltran-Galindo J. Improve the HVAC contribution in wind power smoothing. Electr Power Syst Res Jun. 2019;171:219–29. doi: https://doi.org/10.1016/J.EPSR.2019.01.042.
[8] Ren Y, Yao X, Liu D, Qiao R, Zhang L, Zhang K, et al. Optimal design of hydro-wind-PV multi-energy complementary systems considering smooth power output. Sustain Energy Technol Assessments 2022;50:101832.
[9] Zhu Y, Guo Y, Wang Z, Wei Z. Kinetic energy based output power smoothing control and parameters design for PMSG-WECSs. Int J Electr Power Energy Syst Oct. 2021;131:. doi: https://doi.org/10.1016/J.IJEPES.2021.107077107077.
[10] Zhu Y, Wang Z, Guo X, Wei Z. An improved kinetic energy control strategy for power smoothing of PMSG-WECS based on low pass filter and fuzzy logic controller. Electr Power Syst Res Jan. 2023;214:. doi: https://doi.org/10.1016/J.EPSR.2022.108816108816.
[11] Karimpour M, Schmid R, Tan Y. Exact output regulation for wind turbine active power control. Control Eng Pract Sep. 2021;114:. doi: https://doi.org/10.1016/J.CONENGPRAC.2021.104862104862.
[12] Wakui T, Nagamura A, Yokoyama R. Stabilization of power output and platform motion of a floating offshore wind turbine-generator system using model predictive control based on previewed disturbances. Renew Energy Aug. 2021;173:105–27. doi: https://doi.org/10.1016/J.RENENE.2021.03.112.
[13] Ma L, Xie L, Ye L, Ye J, Ma W. A wind power smoothing strategy based on two-layer model algorithm control. J Energy Storage Apr. 2023;60:. doi: https://doi.org/10.1016/J.EST.2023.106617106617.
[14] Xu Y, Xu Y, Huang Y. Generation of typical operation curves for hydrogen storage applied to the wind power fluctuation smoothing mode. Glob Energy Interconnect Aug. 2022;5(4):353–61. doi: https://doi.org/10.1016/J.GLOEI.2022.08.002.
[15] de Siqueira LMS, Peng W. Control strategy to smooth wind power output using battery energy storage system: A review. J Energy Storage Mar. 2021;35:. doi: https://doi.org/10.1016/J.EST.2021.102252102252.

[16] Lin L, Jia Y, Ma M, Jin X, Zhu L, Luo H. Long-term stable operation control method of dual-battery energy storage system for smoothing wind power fluctuations. Int J Electr Power Energy Syst Jul. 2021;129:. doi: https://doi.org/10.1016/J.IJEPES.2021.106878106878.
[17] Hou T, Fang R, Yang D, Zhang W, Tang J. Energy storage system optimization based on a multi-time scale decomposition-coordination algorithm for wind-ESS systems. Sustain Energy Technol Assessments Feb. 2022;49:. doi: https://doi.org/10.1016/J.SETA.2021.101645101645.
[18] Cao M, Xu Q, Qin X, Cai J. Battery energy storage sizing based on a model predictive control strategy with operational constraints to smooth the wind power. Int J Electr Power Energy Syst Feb. 2020;115:. doi: https://doi.org/10.1016/J.IJEPES.2019.105471105471.
[19] Wang X, Zhou J, Qin B, Guo L. Coordinated control of wind turbine and hybrid energy storage system based on multi-agent deep reinforcement learning for wind power smoothing. J Energy Storage Jan. 2023;57:. doi: https://doi.org/10.1016/J.EST.2022.106297106297.
[20] Sun Y, Pei W, Jia D, Zhang G, Wang H, Zhao L, et al. Application of integrated energy storage system in wind power fluctuation mitigation. J Energy Storage 2020;32:101835.
[21] Yadlapalli RT, Alla RKR, Kandipati R, Kotapati A. Super capacitors for energy storage: Progress, applications and challenges. J Energy Storage May 2022;49:. doi: https://doi.org/10.1016/J.EST.2022.104194104194.
[22] Darvish Falehi A, Torkaman H. Promoted supercapacitor control scheme based on robust fractional-order super-twisting sliding mode control for dynamic voltage restorer to enhance FRT and PQ capabilities of DFIG-based wind turbine. J Energy Storage Oct. 2021;42:. doi: https://doi.org/10.1016/J.EST.2021.102983102983.
[23] de Carvalho WC, Bataglioli RP, Fernandes RAS, Coury DV. Fuzzy-based approach for power smoothing of a full-converter wind turbine generator using a supercapacitor energy storage. Electr Power Syst Res Jul. 2020;184:. doi: https://doi.org/10.1016/J.EPSR.2020.106287106287.
[24] Kumar AW, Ud din Mufti M, Zargar MY. Fuzzy based virtual inertia emulation in a multi-area wind penetrated power system using adaptive predictive control based flywheel storage. Sustain Energy Technol Assessments 2022;53:102515.
[25] Al Afif R, Ayed Y, Maaitah ON. Feasibility and optimal sizing analysis of hybrid renewable energy systems: A case study of Al-Karak, Jordan. Renew Energy Mar. 2023;204:229–49. doi: https://doi.org/10.1016/J.RENENE.2022.12.109.
[26] Moschos I, Koltsaklis N, Parisses C, Christoforidis GC. A positive/negative average real variability index and techno-economic analysis of a hybrid energy storage system. J Energy Storage May 2023;61:. doi: https://doi.org/10.1016/J.EST.2023.106751106751.
[27] Mughees N, Jaffery MH, Jawad M. A new predictive control strategy for improving operating performance of a permanent magnet synchronous generator-based wind energy and superconducting magnetic energy storage hybrid system integrated with grid. J Energy Storage Nov. 2022;55:. doi: https://doi.org/10.1016/J.EST.2022.105515105515.
[28] Chen X, Zhang M, Jiang S, Gou H, Zhou P, Yang R, et al. Energy reliability enhancement of a data center/wind hybrid DC network using superconducting magnetic energy storage. Energy 2023;263:125622.
[29] Kotb KM, Elmorshedy MF, Salama HS, Dán A. Enriching the stability of solar/wind DC microgrids using battery and superconducting magnetic energy storage based fuzzy logic control. J Energy Storage Jan. 2022;45:. doi: https://doi.org/10.1016/J.EST.2021.103751103751.
[30] Tayaba S, Sethi H, Shahid H, Malik R, Ikram M, Ali S, et al. Silicon-Germanium and carbon-based superconductors for electronic, industrial, and medical applications. Mater Sci Eng B 2023;290:116332.
[31] Herbirowo S, Priyanto Utomo E, Feronika Tinambunan D, Sinuhaji P, Sofyan N, Herman Yuwono A, et al. Properties of low-cost MgB2 superconducting wires fabricated by high reduction cold rolling. Mater Today Proc 2023. doi: https://doi.org/10.1016/J.MATPR.2023.01.250.
[32] Boudia A, Messalti S, Harrag A, Boukhnifer M. New hybrid photovoltaic system connected to superconducting magnetic energy storage controlled by PID-fuzzy controller. Energy Convers Manag Sep. 2021;244:. doi: https://doi.org/10.1016/J.ENCONMAN.2021.114435114435.
[33] Muyeen SM, Hasanien HM, Al-Durra A. Transient stability enhancement of wind farms connected to a multi-machine power system by using an adaptive ANN-controlled SMES. Energy Convers Manag Feb. 2014;78:412–20. doi: https://doi.org/10.1016/J.ENCONMAN.2013.10.039.
[34] Jamsheed F, Iqbal SJ. A Neuro-Adaptive Control Scheme to Improve Dynamic Stability of Wind Power System using Battery Energy Storage. IFAC-PapersOnLine Jan. 2022;55(9):164–9. doi: https://doi.org/10.1016/J.IFACOL.2022.07.029.
[35] Hasanien HM, Matar M. Water cycle algorithm-based optimal control strategy for efficient operation of an autonomous microgrid. IET Gener Transm Distrib Nov. 2018;12(21):5739–46. doi: https://doi.org/10.1049/IET-GTD.2018.5715.
[36] Hasanien HM. Performance improvement of photovoltaic power systems using an optimal control strategy based on whale optimization algorithm. Electr Power Syst Res Apr. 2018;157:168–76. doi: https://doi.org/10.1016/J.EPSR.2017.12.019.
[37] Qais MH, Hasanien HM, Alghuwainem S. Enhanced salp swarm algorithm: Application to variable speed wind generators. Eng Appl Artif Intell Apr. 2019;80:82–96. doi: https://doi.org/10.1016/J.ENGAPPAI.2019.01.011.
[38] Qais MH, Hasanien HM, Alghuwainem S. Augmented grey wolf optimizer for grid-connected PMSG-based wind energy conversion systems. Appl Soft Comput Aug. 2018;69:504–15. doi: https://doi.org/10.1016/J.ASOC.2018.05.006.
[39] Qais MH, Hasanien HM, Alghuwainem S. Optimal Transient Search Algorithm-Based PI Controllers for Enhancing Low Voltage Ride-Through Ability of Grid-Linked PMSG-Based Wind Turbine. Electronics 2020;9(11):1807.
[40] Jannati M, Hosseinian SH, Vahidi B, Li G-J. ADALINE (ADAptive Linear NEuron)-based coordinated control for wind power fluctuations smoothing with reduced BESS (battery energy storage system) capacity. Energy 2016;101:1–8.
[41] Hasanien HM, Muyeen SM. Affine projection algorithm based adaptive control scheme for operation of variable-speed wind generator. IET Gener Transm Distrib Dec. 2015;9(16):2611–6. doi: https://doi.org/10.1049/IET-GTD.2014.1146.
[42] Hasanien HM. An Adaptive Control Strategy for Low Voltage Ride Through Capability Enhancement of Grid-Connected Photovoltaic Power Plants. IEEE Trans Power Syst Jul. 2016;31(4):3230–7. doi: https://doi.org/10.1109/TPWRS.2015.2466618.
[43] Xia X, Sun S, Jing X, Huang H. A variable parameter efficient μ-law improved proportionate affine projection algorithm. CCIS2011 - Proc. 2011 IEEE Int. Conf. Cloud Comput. Intell. Syst., pp. 577–581, 2011, doi: 10.1109/CCIS.2011.6045135.
[44] Gil-Cacho JM, Signoretto M, Van Waterschoot T, Moonen M, Jensen SH. Nonlinear acoustic echo cancellation based on a sliding-window leaky kernel affine projection algorithm. IEEE Trans Audio, Speech Lang Process 2013;21(9):1867–78. doi: https://doi.org/10.1109/TASL.2013.2260742.
[45] Diniz PSR. Adaptive filtering: Algorithms and practical implementation. Adapt Filter Algorithms Pract Implement Nov. 2013;9781461441069:1–652. doi: https://doi.org/10.1007/978-1-4614-4106-9/COVER.
[46] Zayyani H. Continuous mixed p-norm adaptive algorithm for system identification. IEEE Signal Process Lett 2014;21(9):1108–10. doi: https://doi.org/10.1109/LSP.2014.2325495.
[47] Soliman MA, Hasanien HM, Al-Durra A, Alsaidan I. A novel adaptive control method for performance enhancement of grid-connected variable-speed wind generators. IEEE Access 2020;8:82617–29. doi: https://doi.org/10.1109/ACCESS.2020.2991689.
[48] Qais MH, Hasanien HM, Alghuwainem S. A novel LMSRE-based adaptive PI control scheme for grid-integrated PMSG-based variable-speed wind turbine. Int J Electr Power Energy Syst Feb. 2021;125:. doi: https://doi.org/10.1016/J.IJEPES.2020.106505106505.
[49] Zahra H, Hadi Z, Mohammad SEA. A robust subband adaptive filter algorithm for sparse and block-sparse systems identification. J Syst Eng Electron Apr. 2021;32(2):487–97. doi: https://doi.org/10.23919/JSEE.2021.000041.
[50] "EMTDC User's Guide v4.6 | PSCAD." https://www.pscad.com/knowledge-base/article/163 [accessed Apr. 01, 2023].
[51] Katagiri T, Nakabayashi H, Nijo Y, Tamada T, Noda T, Hirano N, et al. Field test result of 10MVA/20MJ SMES for load fluctuation compensation. IEEE Trans Appl Supercond 2009;19(3):1993–8.
[52] Chambers JA, Tanrikulu O, Constantinides AG. Least mean mixed-norm adaptive filtering. Electron Lett Sep. 1994;30(19):1574–5. doi: https://doi.org/10.1049/EL:19941060.
[53] Chambers J, Avlonitis A. A robust mixed-norm adaptive filter algorithm. IEEE Signal Process Lett 1997;4(2):46–8. doi: https://doi.org/10.1109/97.554469.
[54] Papoulis EV, Stathaki T. A Normalized Robust Mixed-Norm Adaptive Algorithm for System Identification. IEEE Signal Process Lett Jan. 2004;11(1):56–9. doi: https://doi.org/10.1109/LSP.2003.819353.
[55] Kivinen J, Warmuth MK, Hassibi B. The p-norm generalization of the LMS algorithm for adaptive filtering. IEEE Trans Signal Process May 2006;54(5):1782–93. doi: https://doi.org/10.1109/TSP.2006.872551.

Rania A. Turky received his B.Sc. and M.Sc. degrees in Electrical Power Engineering from Ain Shams University, Faculty of Engineering, Cairo, Egypt, in 2004 and 2010, respectively. She is now pursuing PhD degree at Ain Shams University. Her research interests include modern control techniques, power systems dynamics and control, energy storage systems, renewable energy systems, and smart grid.

Tarek Saad Abdel-Salam got his B.Sc. and M.Sc. degrees from Ain Shams University, Cairo, Egypt in the Department of Electrical Power and Machines 1980 and 1986 respectively. Got his Ph.D. degree from University of Windsor, Windsor, Ontario, Canada, 1994 in the area of Power Loss Reduction on the Power Distribution Systems. He is a technical committee member for many national and international conferences, national and international journals. He works as a consultant engineer for many projects in Egypt and Saudi Arabia. Currently, he is a professor emeritus at Ain Shams University.

Hany M. Hasanien (M 09, SM 11) received his B.Sc., M. Sc. and Ph.D. degrees in Electrical Engineering from Ain Shams University, Faculty of Engineering, Cairo, Egypt, in 1999, 2004, and 2007, respectively. From 2008 to 2011, he was a Joint Researcher with Kitami Institute of Technology, Kitami, Japan. From 2012 to 2015, he was Associate Professor at College of Engineering, King Saud University, Riyadh, Saudi Arabia. Currently, he is Professor at the Electrical Power and Machines Department, Faculty of Engineering, Ain Shams University. His research interests include modern control techniques, power systems dynamics and control, energy storage systems, renewable energy systems, and smart grid. Prof. Hasanien is an Editorial Board Member of *Electric Power Components and Systems Journal*. He is Subject Editor of IET Renewable Power Generation, Frontiers in Energy Research and Electronics MDPI. He has authored, co-authored, and edited three books in the field of electric machines and renewable energy. He has published more than 250 papers in international journals and conferences. His biography has been included in *Marquis Who's Who in the world* for its 28 edition, 2011. He was awarded Encouraging Egypt Award for Engineering Sciences in 2012. He was awarded Institutions Egypt Award for Invention and Innovation of Renewable Energy Systems Development in 2014. He was awarded the Superiority Egypt Award for Engineering Sciences in 2019. He was the IEEE PES Egypt Chapter Chair (2020-2022). Currently, he is Editor in Chief of Ain Shams Engineering Journal, Elsevier. Currently, he is a Courtesy Professor at Department of Electrical and Computer Engineering, Florida International University, Miami, FL 33174 USA.

Mohammed Alharbi received the B.S. degree in electrical engineering from King Saud University, Riyadh, Saudi Arabia, in 2010, and the M.S. degree in electrical engineering from the Missouri University of Science and Technology, Rolla, MO, USA, in 2014, the Ph.D. degree in electrical engineering from the North Carolina State University, Raleigh, NC, USA, in 2020. He was a Teaching Assistant with King Saud University from September 2010 till May 2011. He was a project engineer at the FREEDM Systems Center in the North Carolina State University, Raleigh, NC, USA from January 2016 till December 2019, where he was involved in designing and constructing a modular multi-level converter for control validations. In August 2020, he joined the Department of Electrical Engineering, King Saud University, Riyadh, Saudi Arabia, where he is currently an Assistant Professor. His research interests include medium voltage and high-power converters, modular multi-level converter (MMC) controls, multi-terminal HVdc systems, and grid integration of renewable energy systems.

Zia Ullah (Member, IEEE); Dr. Zia Ullah received a Ph.D. degree in Electrical Engineering from the Huazhong University of Science and Technology (HUST), Wuhan, China, in 2020.. Currently, he is working as a Postdoctoral Research Fellow with the State Key Laboratory of Advanced Electromagnetic Engineering and Technology, at school of Electrical and Electronic Engineering, HUST. His research interests include power system optimization, intelligent power distribution system, distribution system planning with RES, operation and control, EV-integrated distribution networks optimization, EV charging station designing, and EV scheduling optimization.

Dr. S.M. Muyeen (S'03–M'08–SM'12) is a full professor in the Electrical Engineering Department of Qatar University. He received his B.Sc. Eng. Degree from Rajshahi University of Engineering and Technology (RUET), Bangladesh, formerly known as Rajshahi Institute of Technology, in 2000 and M. Eng. and Ph.D. Degrees from Kitami Institute of Technology, Japan, in 2005 and 2008, respectively, all in Electrical and Electronic Engineering. His research interests are power system stability and control, electrical machine, FACTS, energy storage system (ESS), Renewable Energy, and HVDC system. He has been a Keynote Speaker and an Invited Speaker at many international conferences, workshops, and universities. He has published more than 350+ articles in different journals and international conferences. He has published seven books as an author or editor. He is serving as Editor/Associate Editor for many prestigious Journals from IEEE, IET, and other publishers, including IEEE Transactions on Energy Conversion, IEEE Power Engineering Letters, IET Renewable Power Generation and IET Generation, Transmission & Distribution, etc. Dr. Muyeen is a senior member of IEEE, Chartered Professional Engineers, Australia, and a Fellow of Engineers Australia.

Amr Magdy Abdin is Associate professor at the Faculty of Engineering Ain Shams University. Amr received his doctor of philosophy degree in 2012 and now he is the Unit Head for the Energy and Renewable Energy program managing all the technical and educational aspects of the program, Dual-Degree collaboration with the University of East London. He is a Technical Educational Consultant at Schneider Electric (NEAL). A multinational company in the field of energy management and electrical distribution components. Amr is now Leading the educational initiative program with all Egyptian universities to enhance the students' capabilities and industrial engagement and also providing technical training for Schneider employees, customers and consultants. He leads Exchanges, Training, Mentorship and Scholarships at the Center of Excellence for Energy Research, Education and Entrepreneurship (COE-Energy). Funded by USAID and in collaboration with Arizona State University. He is responsible for Visiting Faculty Scholars to ASU, Internship Placements with Private Sector, Graduate Students Conducting Research on Joint Egypt-ASU projects at ASU for a one-semester exchange.